Fracture Mechanics of Concrete and Concrete Structures - High Performance, Fiber Reinforced Concrete, Special Loadings and Structural Applications- B. H. Oh, et al. (eds)
© 2010 Korea Concrete Institute, ISBN 978-89-5708-182-2

Behaviors of FRP sheet reinforced concrete to impact and static loading

K. –H. Min, S. –H. Cho, D. –Y. Yoo & Y. –S. Yoon
Korea University

ABSTRACT: In this study, in order to assess the flexural reinforcing effects of fiber reinforced polymer (FRP) sheets for static and impact loading, flexural performances were tested with variables of types of fiber, sheets, and reinforcing methods. With the GFRP, CFRP, and AFRP sheets, 100×100×400 mm prismatic specimens were retrofitted to the bottom surface, to the U-strip at the center, and both ways. Flexural loading static tests and drop weight impact tests were carried out. The U-strip reinforced specimens did not increase the flexural strength. However specimens with a reinforced bottom surface and the specimens doubly reinforced with CFRP and AFRP showed much higher strength than non-reinforced specimens. Because the U-strip reinforced specimens had the same direction as the cracks, they were governed only by the strength of resins. However, the specimens with a reinforced bottom surface and the doubly reinforced specimens showed much higher energy absorptions.

1 INTRODUCTION

Today, advanced research and the discovery of more practical uses for FRPs (fiber reinforced plastics or polymers) to retrofit and rehabilitate concrete structures have progressed. Recently, construction structures demand a higher resistance to impacts, blasts, earthquakes, and extreme fires (Banthia *et al*. 1989, Bindiganavile *et al.* 2002, Min *et al.* 2009). Because of the significant benefits with high strain rate loads, many researchers are paying attention to FRPs for the reinforcement of construction structures (Buchan & Chen 2006, Malvar *et al.* 2007, Silva & Lu 2007).

The ACI 440 assumes only two failure modes for design calculations: compressive failure of the concrete and failure of the FRP strengthening system (ACI 2002, Bank 2006). However, the actual FRP products are skill-dependent and the quality is not uniform. Apart from the cost, the most essential problem in the FRP system is the "bond" between the FRP and concrete. Typical failure modes of FRP-plates or sheet reinforced RC beams are classified as FRP rupture, crushing of compressive concrete, shear failure, concrete cover separation, plate-end interfacial debonding, intermediate flexural crack-induced interfacial debonding, intermediate flexural shear crack-induced interfacial debonding (Teng *et al*. 2002). Also, almost all failure modes show a brittle manner.

Therefore, in this study, in order to observe the behaviors of FRP strengthened concrete specimens for impact and static loads, flexural tests were carried out with specimens of glass fiber reinforced polymer (GFRP), carbon fiber reinforced polymer (CFRP), and aramid fiber reinforced polymer (AFRP).

2 MATERIALS AND VARIABLES

Table 1 shows the mix proportions for 30 MPa design strength concrete used in this study. The fineness and specific gravity of the ordinary Portland cement were 348.3 m^2/kg and 3.15, respectively. Aggregates were crushed gravels with a maximum size of 20 mm and a fineness modulus of 6.56, and sea sands with a fineness modulus of 2.55. In order to achieve workability, a liquid type poly-carboxylic high-range AE water reducer was injected.

Table 1. Mix proportions of concrete.

W/C	S/a	Unit weight (kg/m3)				
(%)	(%)	Water	Cement	Fine agg.	Coarse agg.	Adm.
60	45	350	583	544	667	2.9

In this study, three FRPs (GFRP, CFRP, and AFRP) and two resins (epoxy, polyester) were used. The mechanical properties of fibers and resins are summarized in Table 2. Also, variables of the tests are summarized in Table 3.

Compared to the epoxy, the polyester has a lower strength, and is therefore adequate only for GFRP. In this study, polyester resin was used with GFRP, while epoxy was used with the three FRPs. The carbon and aramid sheets were unidirectional (UD) only. On the GFRPs, three sheets (unidirectional, woven roving (WR), and chopped strand (CS)) and two resins were applied. Figures of the three sheets are shown in Table 3. As illustrated in Figure 1,

three types of reinforcing (bottom strengthening, center U-strip, and reinforced both) were utilized.

For the flexural load, concrete specimens with the dimensions of 100×100×400 mm were made. The mixtures were cast into steel molds (for flexural specimens) and plastic molds (for cylinder specimens) with modest vibration. After casting, the specimens were covered with plastic sheets and were then left in the casting room for 24 hours at 20±2°C. They were then demolded and stored in water at 20±3°C until tested. 14 days after casting, the FRPs were adhered and then cured for 14 days more at 50% relative humidity and at a temperature of 20°C.

Table 2. Properties of fibers and resins.

Fiber	Glass	Carbon	Aramid
Tensile strength (MPa)	2,300	4,900	2,880
Elastic modulus (GPa)	76	230	100
Ultimate strain (%)	3.0	2.1	2.9
Thickness (mm)	0.350	0.111	0.194
Resin	**Epoxy**		**Polyester**
Tensile strength (MPa)	90		65
Elastic modulus (GPa, tensile)	3.0		4.0
Ultimate strain (%)	8.0		2.5
Density (kg/m^3)	1200		1200

Table 3. Test variables.

Variable	Detail	Notation
Fiber	Glass	GFRP
	Carbon	CFRP
	Aramid	AFRP
Resin*	Epoxy	EPX
	Polyester	PE
Sheet*	Unidirectional	UD
	Woven roving	WR
	Chopped strand	CS


UD


WR


CS

*Variables of resins and sheets were only available for GFRPs.

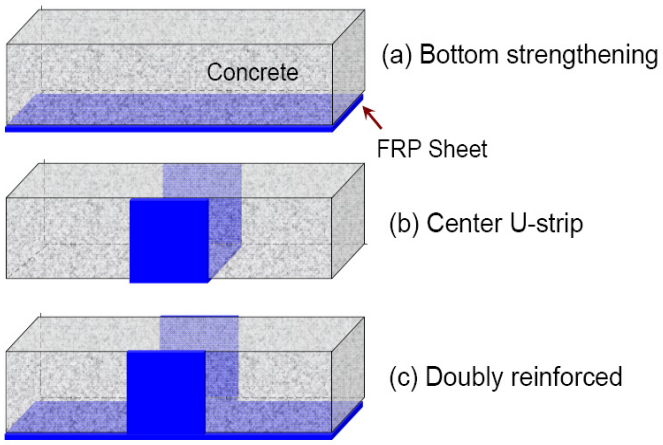

Figure 1. Specimens reinforced with FRP sheets.

3 EXPERIMENTAL PROGRAM

3.1 *Static flexural tests*

The flexural strength was measured according to the four point flexural test specified in the ASTM C 78. For flexural specimens, the loading was applied gradually using a 2,700kN capacity UTM (universal testing machine) under displacement control at a loading rate of 0.01 mm/s. The deflection at the center of both sides was then measured with two LVDTs (linear variable differential transformers) as shown below Figure 2.

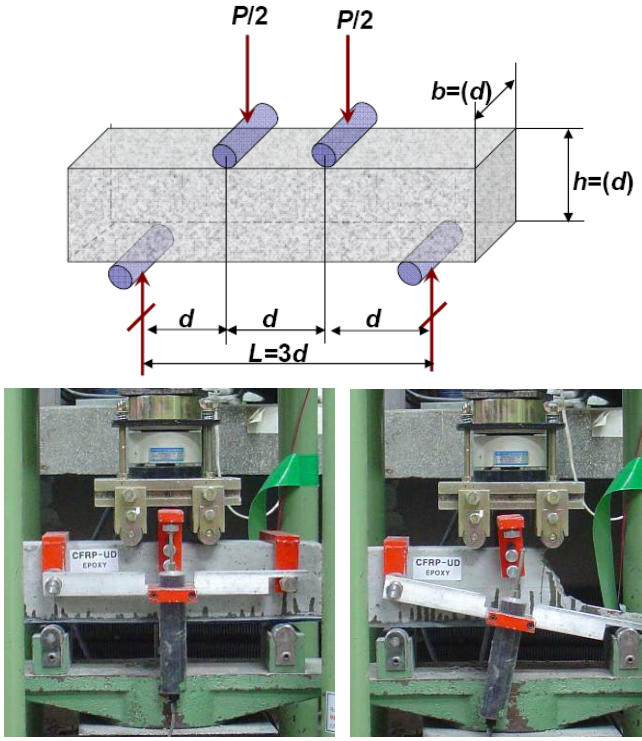

Figure 2. Setup for static flexural tests.

3.2 *Impact tests*

Impact tests were carried out with a drop weight test machine that has a maximum capacity of about 1000 Joules (Fig. 3). Considering the high energy dissipation ability of retrofitted specimens, a 33.62 kg weight was dropped with air pressure along a 0.7 m clear height. The span of each specimen was 300 mm. The load cell in the tub, with the attached speedometer, measured the impact load and velocity. Then the computer calculated the impact energy (J), impact velocity (m/sec), maximum load (kN), total energy (J), and energy at failure (J), etc.

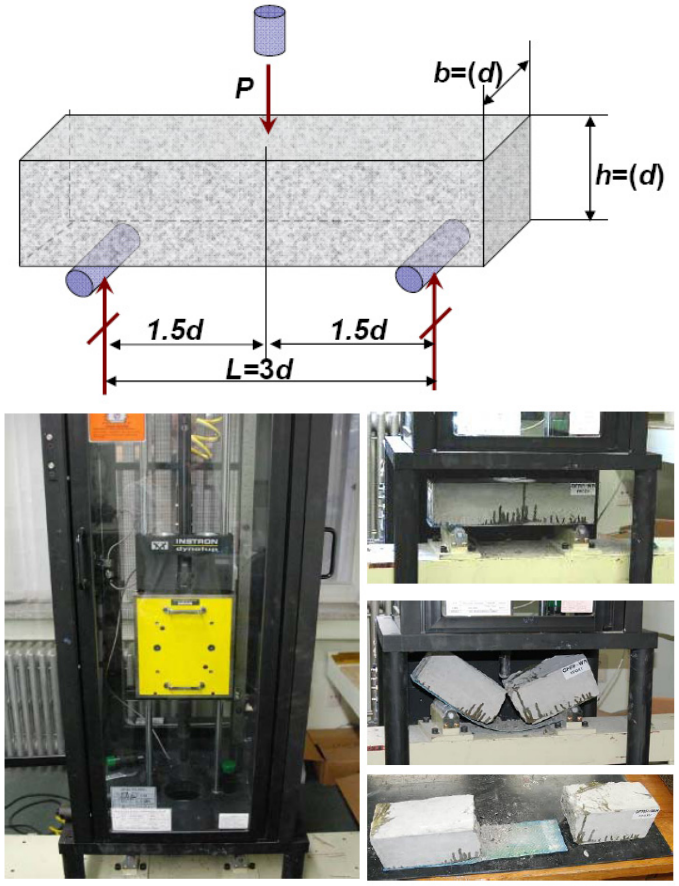

Figure 3. Setup of impact tests.

4 RESULTS AND DISCUSSIONS

4.1 *Static flexural tests*

The results of the static flexural tests are summarized in Table 4. Figures 4 to 6 show the load-deflection relationships of bottom strengthened specimens in the static tests. Due to the low bond strength of polyester, the maximum load and ultimate strength of the PE series of GFRPs were marginally more improved than the plain concrete specimen (NC) and showed softening after peak load. However, in contrast to plain concrete, the behaviors were less brittle. While the strength of the EPX series of GFRPs marginally increased, the toughness increased significantly.

The increased strength by the chopped strand (CS) mat, which had no direction of fiber, were lower than those by the woven roving (WR) and unidirectional (UD) fabrics. Also, the unidirectional fabric reinforced members failed and showed less toughness than the CS and WR specimens'. The CFRP with epoxy resin performed better than other FRP systems for the strength and stiffness. The enhanced strength and stiffness of AFRP reinforced specimens were lower than those of the CFRP reinforced specimens but had higher final deflections.

As shown in Figures 7 and 8, strengthening the U-strip in the center did not enhance the flexural strength, because the fiber arrangement was the same as the crack propagating directions. Hence, doubly reinforced specimens showed a similar strength to bottom strengthened specimens (Figs. 9 & 10). Although they showed a lower stiffness than CFRP's cases, the doubly reinforced with AFRP showed a similar strength to the CFRP reinforced specimens.

Table 4. Results of static flexural tests.

Specimen		Maximum load (kN)	Ultimate strength (MPa)
NC		22.06	6.62
Bottom strengthening	GFRP-CS-PE	25.01	7.50
	GFRP-WR-PE	25.66	7.70
	GFRP-UD-PE	31.61	9.48
	GFRP-CS-EPX	45.77	13.73
	GFRP-WR-EPX	54.80	16.44
	GFRP-UD-EPX	60.85	18.25
	CFRP	92.26	27.68
	AFRP	69.15	20.74
Center U-strip	GFRP-CS-EPX	29.89	8.97
	GFRP-WR-EPX	32.94	9.88
	GFRP-UD-EPX	28.31	8.49
	CFRP	21.43	6.43
	AFRP	24.33	7.30
Doubly reinforced	GFRP-CS-EPX	45.79	13.74
	GFRP-WR-EPX	52.22	15.67
	GFRP-UD-EPX	72.47	21.74
	CFRP	86.82	26.05
	AFRP	80.31	24.09

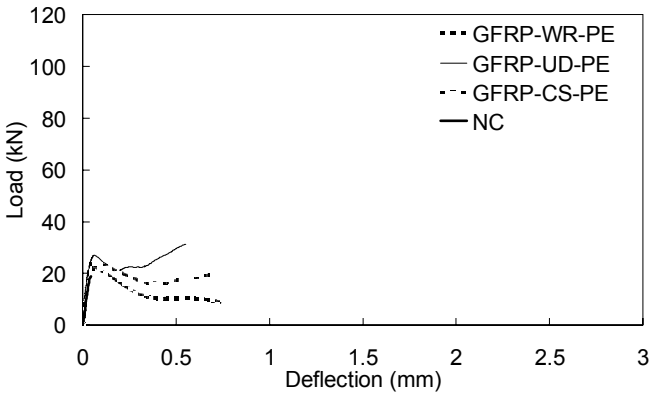

Figure 4. Static load-deflection relationship of bottom strengthened specimens using polyester.

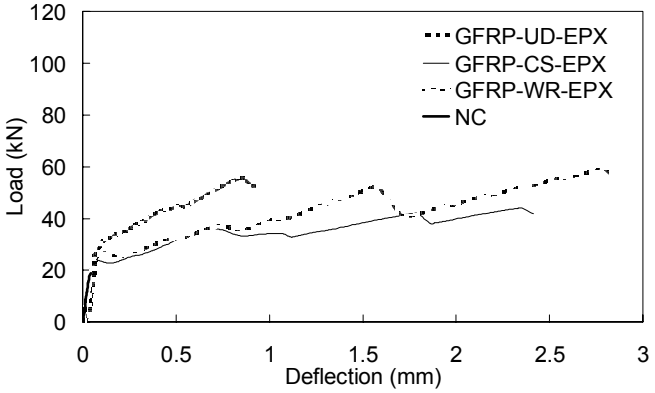

Figure 5. Static load-deflection relationship of bottom strengthened specimens using epoxy.

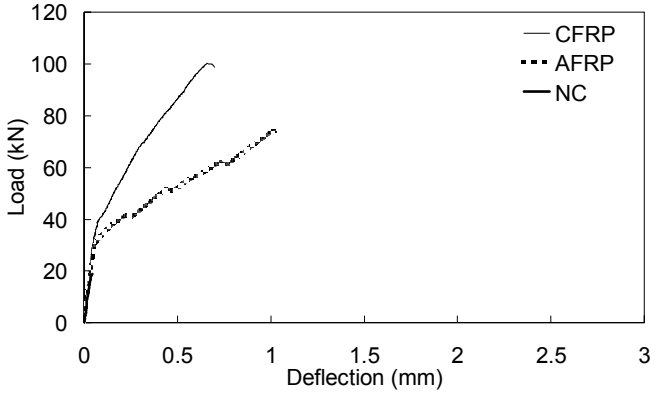

Figure 6. Static load-deflection relationship of bottom strengthened specimens with CFRP and AFRP.

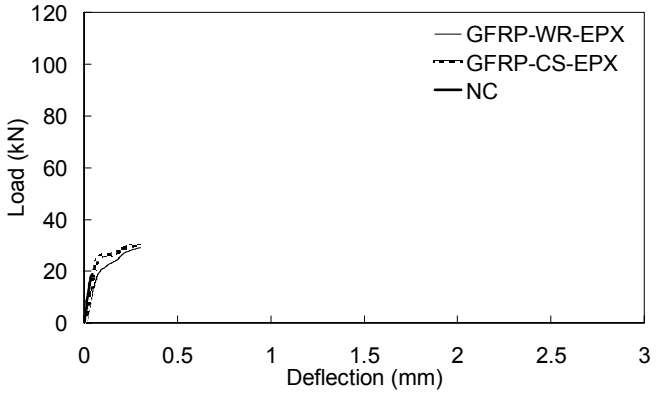

Figure 7. Static load-deflection relationship of specimens reinforced with GFRP U-strip.

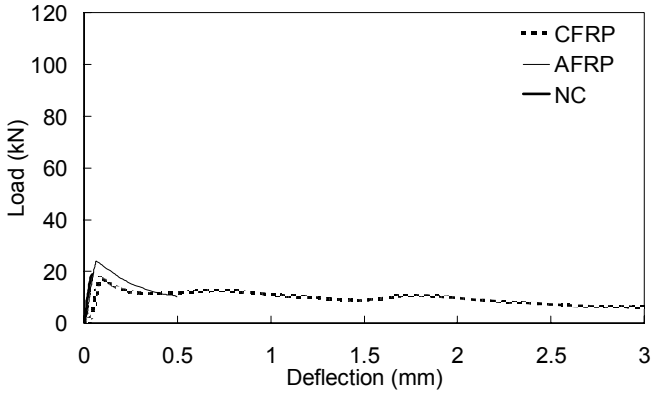

Figure 8. Static load-deflection relationship of specimens reinforced with CFRP and AFRP U-strip.

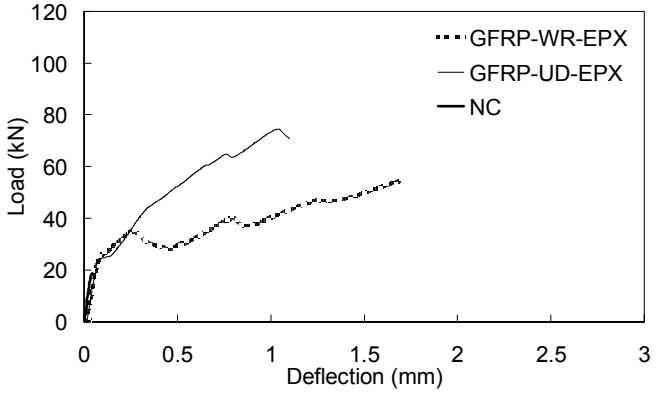

Figure 9. Static load-deflection relationship of specimens doubly reinforced with GFRP.

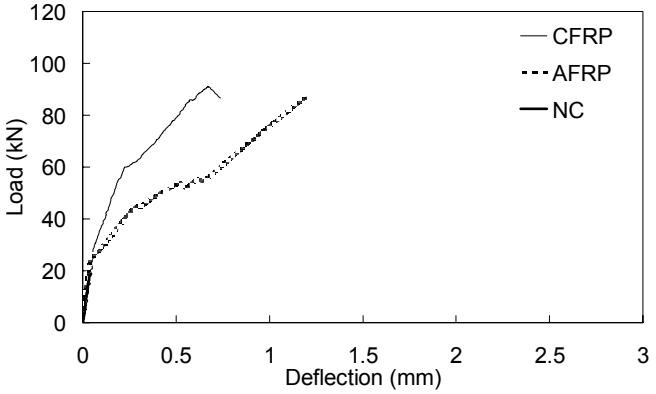

Figure 10. Static load-deflection relationship of specimens doubly reinforced with CFRP and AFRP.

4.2 *Impact tests*

The results of the impact tests are summarized in Table 5. Figures 11 to 17 show the load-deflection relationships of specimens in the impact tests. Note that the graphs do not show average values but rather show typical cases of each series. In the impact tests, in order to measure the total failure energy, the drop weight energy should be very high; this means that the specimens can be demolished with a one shot loading. Loads could be measured by the load cell in the tub. At the applied load, within a very short duration, the specimens vibrate and the contents of the tub penetrate a thin layer of the specimens. Hence the load and deflection curves are not regular but swayable. In addition, there were relatively larger deviations for the same series.

Although not sufficiently reinforced members, the specimens reinforced with the U-strip and

Table 5. Results of impact tests.

Specimen	Max. Load (kN)	Defl. at max. load (mm)	Total energy (J)
NC	49.04	1.98	140.72
Bottom strengthening			
GFRP-CS-PE	62.51	2.76	199.10
GFRP-WR-PE	65.66	2.86	192.81
GFRP-UD-PE	45.69	–	–
GFRP-CS-EPX	67.99	2.68	241.17
GFRP-WR-EPX	63.84	2.00	391.49
GFRP-UD-EPX	70.30	5.14	308.88
CFRP: 1st strike	63.37	4.16	535.03
2nd strike	73.34	6.32	377.95
AFRP	66.48	4.23	400.80
Center U-strip			
GFRP-CS-EPX	67.69	4.10	241.94
GFRP-UD-EPX	60.29	2.53	168.48
CFRP	58.94	3.31	186.98
AFRP	66.14	2.99	187.21
Doubly reinforced			
GFRP-CS-EPX	72.76	4.63	283.48
GFRP-UD-EPX	65.26	2.81	576.13
CFRP	66.17	2.78	362.57
AFRP: 1st strike	71.59	9.23	524.54
2nd strike	50.02	6.89	208.77

bonded with the polyester, had higher maximum loads and they performed with small increases of deflections and toughness as can be shown in Figures 11, 14 and 15. However, FRP strengthening is available for the energy dissipating capacities. Measured maximum load and total energy in the impact tests were increased up to 45 and 300%, respectively. Some specimens strengthened with CFRP and AFRP did not fail in one shot, and specimens doubly reinforced with CFRP and AFRP failed along the longitudinal direction.

The specimens under impact loads behaved with larger deformation than those under static loads.

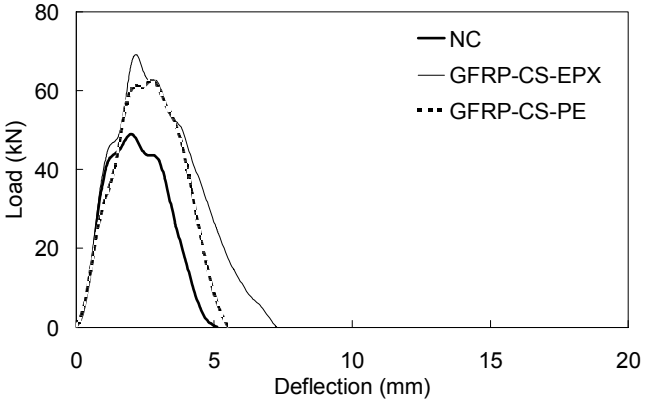

Figure 11. Impact load-deflection relationship of bottom strengthened specimens using epoxy.

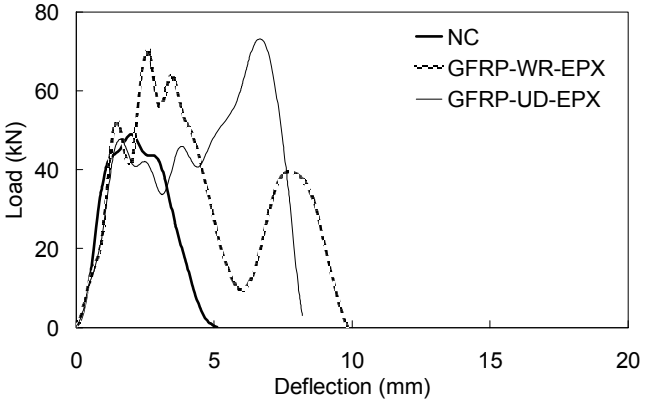

Figure 12. Impact load-deflection relationship of bottom strengthened specimens using polyester.

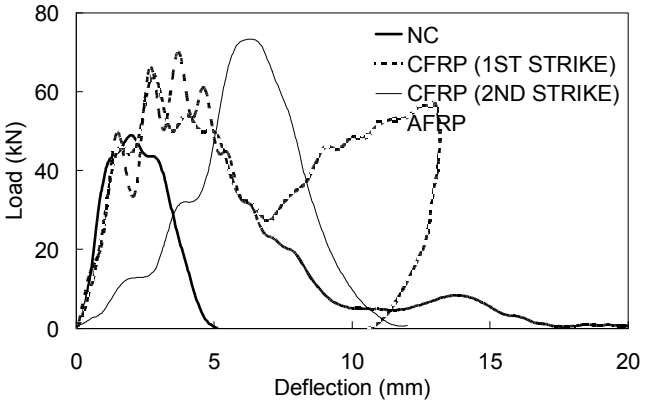

Figure 13. Impact load-deflection relationship of bottom strengthened specimens with CFRP and AFRP.

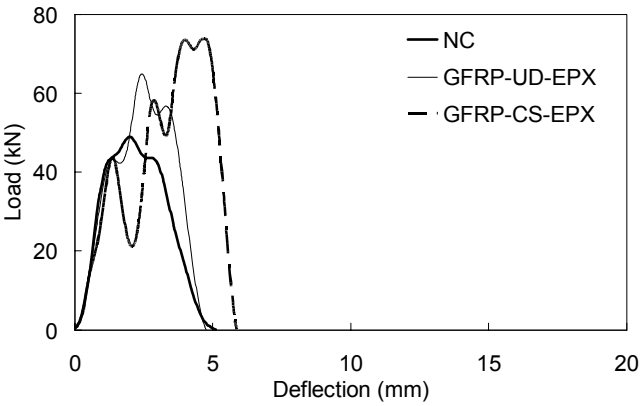

Figure 14. Impact load-deflection relationship of specimens reinforced with GFRP U-strip.

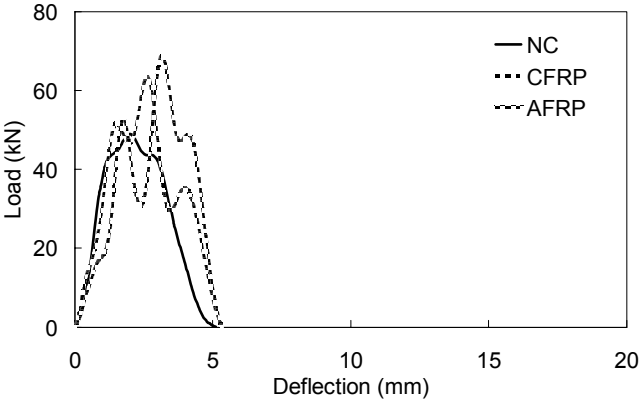

Figure 15. Impact load-deflection relationship of specimens reinforced with CFRP and AFRP U-strip.

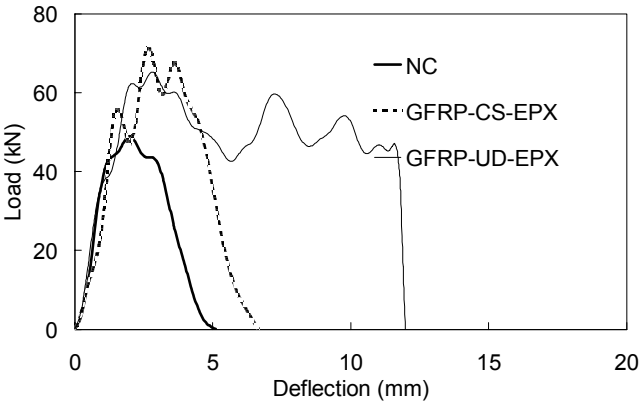

Figure 16. Impact load-deflection relationship of specimens doubly reinforced with GFRP.

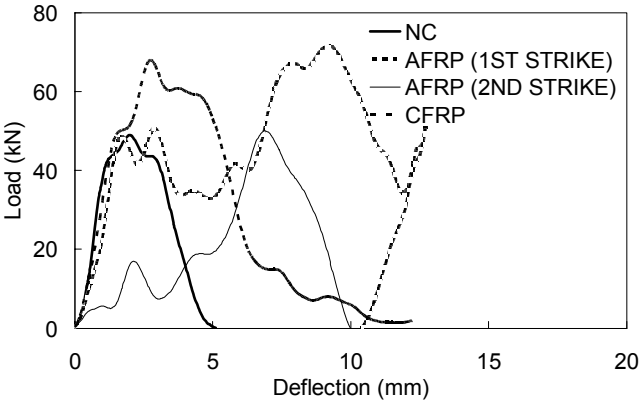

Figure 17. Impact load-deflection relationship of specimens doubly reinforced with CFRP and AFRP.

Every retrofitted specimen deflected more than 2mm at maximum load; even specimens strengthened by CFRP and AFRP that showed 10 mm deflections did not failed. The large deformations provide high energy dissipating capacities for impact loads. As can be seen in Figures 13 and 14, some displacement was recovered for specimens where the member did not fail in one shot displacement recovered.

5 CONCLUSIONS

The following is outline of concluding remarks for this experimental study:

1. The ultimate strength of GFRPs reinforced with polyester resin marginally improved and showed softening after peak load. The enhanced strength by applying the chopped strand mat was less than that by applying the woven roving and unidirectional sheets. The U-strip strengthening in the center did not enhance the flexural strength.
2. The CFRP with epoxy resin showed the most outstanding performance under static load. The enhanced strength and stiffness of the AFRP reinforced specimens were lower than those of the CFRPs.
3. FRP strengthening is available for the energy dissipating capacities under the impact load. Some specimens strengthened with CFRP and AFRP did not fail in one shot, and specimens doubly reinforced with CFRP and AFRP failed along the longitudinal direction.
4. The FRP retrofitted specimens under impact loads behaved with larger deformations, and they demonstrated high energy dissipating capacities under high strain rate loads.

ACKNOWLEDGEMENT

This work was supported by the National Research Foundation of Korea (NRF) grant funded by the Korea government (MEST) (No. 2007-0056796).

REFERENCES

ACI Committee 440. 2002. Guide for the Design and Construction of Externally Bonded FRP Systems for Strengthening Concrete Structures. ACI 440.2R-02. American Concrete Institute. MI.

ASTM C 78. 2007. Standard Test Method for Flexural Strength of Concrete (Using Simple Beam with Third-Point Loading). American Society for Testing and Materials. PA.

Bank, L.C. 2006. Composites for Construction: Structural Design with FRP Materials. NJ: John Wiley & Sons: 214-271.

Banthia, N., Mindess, S., Bentur, A. & Pigeon, M. 1989. Impact Testing of Concrete Using a Drop-weight Impact Machine. Experimental Mechanics. 29(1):63-69.

Bindiganavile, V., Banthia, N. & Aarup, B. 2002. Impact Response of Ultra-High-Strength Fiber-Reinforced Cement Composite. ACI Material Journal. 99(6):543-548.

Buchan, P.A. & Chen, J.F. 2006. Blast Resistance of FRP Composites and Polymer Strengthened Concrete and Masonry Structures – A State-of-the-art Review. Composites: Part B. 38(5-6):509-522.

Malvar, L.J., Crawford, J.E. & Morrill K.B. 2007. Use of Composites to Resist Blast. Journal of Composites for Construction, ASCE. 11(6):601-610.

Min, K.–H., Cho, S.–H., Kim, Y.–W., Shin, H.–O. & Yoon, Y.–S. 2009. Assessment on Impact Resisting Performance of HPFRCCs Using Hybrid PVA Fibers. Structures under Extreme Loading: Proceedings of PROTECT2009. Yokohama: National Defense Academy Protect Workshop.

Silva, P.F. & Lu, B. 2007. Improving the Blast Resistance Capacity of RC Slabs with Innovative Composite Materials. Composite: Part B. 38(5-6):523-534.

Teng, J.G., Chen, J.F., Smith, S.T. & Lam, L. 2002. FRP-Strengthened RC Structures. West Sussex: John Wiley & Sons: 31-46.